Energy dissipation and equivalent damping of RC columns subjected to biaxial bending: An investigation based in experimental results

H. Rodrigues
Civil Engineering Department, University of Aveiro
Faculty of Natural Sciences, Engineering and Technology - Oporto Lusophone University

A. Arêde
Civil Engineering Department, Faculty of Engineering, University of Porto

H. Varum & A.G. Costa
Civil Engineering Department, University of Aveiro

SUMMARY:
The cyclic behaviour of reinforced concrete columns have been object of many experimental studies in the recent past years. However, the experimental studies on the biaxial response of RC columns are still limited. In this paper are presented the main results of an experimental study of 24 full-scale rectangular building columns tested for different loading paths under uniaxial and biaxial conditions. The experimental results are presented and discussed in terms of global behaviour, particularly focusing on the stiffness and strength degradation due to the increasing cyclic demand, and energy dissipation evolution. The equivalent viscous damping was estimated based on the experimental results of the RC columns tested under biaxial loading and empirical expressions are proposed.

Keywords: RC columns; Hysteretic behaviour; Biaxial testing; Energy dissipation; Viscous damping

1. INTRODUCTION

The behaviour of reinforced concrete (RC) elements subjected to axial loading in conjunction with cyclic biaxial bending is recognised as a very important research topic for building structures in earthquake prone regions. Previous experimental work agrees that biaxial horizontal cyclic loading can increase the strength and stiffness degradation, when compared to uniaxial loading. In addition, the failure mechanism of RC columns is found to be highly dependent on the load path and history and strongly affects both the ductility and energy dissipation capacity of the columns (CEB, 1996; Rodrigues *et al.*, 2010).
Energy dissipation is a fundamental structural property of RC elements when subjected to seismic demands. For RC structures designed to accommodate damage without collapse due to a seismic event, the input energy can be dissipated through RC element's hysteretic response, without a significant reduction in strength (Elmenshawi & Brown, 2010). Viscous damping is used to characterise the energy dissipation capacity of RC elements and is one of the key parameters for the application of displacement based design (DBD) methods (Lu & Silva).
Energy dissipation and the equivalent viscous damping have been correlated with displacement ductility for uniaxial stress. The current work intends to compare energy dissipation and equivalent viscous damping on RC columns subjected to uniaxial and biaxial loads. Finally, consideration is given to whether the available formulas relating viscous damping with the displacement ductility that have been proposed for uniaxial demands are applicable to biaxial loading.

2. TEST PROGRAM

In the experimental campaign were tested twenty-four rectangular RC columns with different types of geometric characteristic and reinforcement detailing and were cyclically tested for different loading histories with a constant axial force and under displacement controlled conditions. The column specimens are 1.70m high and are cast in strong square concrete foundation blocks. The cross-section dimensions and the reinforcement detailing are presented in Figure 1. Figure 2 shows the setup adopted for the experimental testing set up. In order to characterise the response of the column specimens, cyclic lateral displacements were imposed at the top of the column with steadily increasing demand levels. Three cycles were repeated for each lateral deformation demand level. This procedure allows for the understanding of the column's behaviour, a comparison between different

tests and provides information for the development and calibration of numerical models, the following nominal peak displacement levels (in mm) were considered: 3, 5, 10, 4, 12, 15, 7, 20, 25, 30, 35, 40, 45, 50, 55, 60, 65, 70, 75, 80.

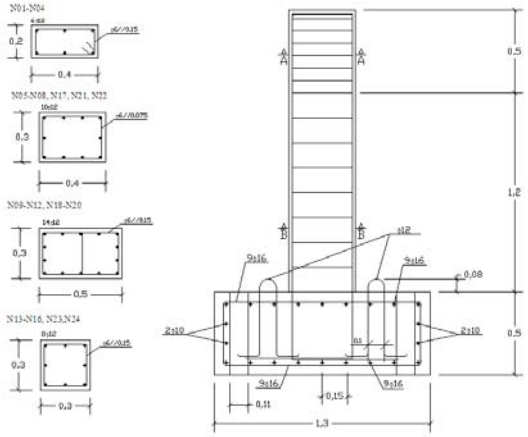

Figure 1–RC column specimen dimensions and reinforcement detailing

Figure 2–Testing setup

Table 1–Specimen specifications and loading characteristics

Series	Column	Geometry [cmxcm]	f_{cm} [MPa]	N [kN]	ν $N/(A_c \cdot f_{cm})$	Displacement path type
1	PB01-N01 PB02-N02 PB12-N03 PB12-N04	20x40	48.35	170	0.04	Uniaxial Strong Uniaxial Weak Cruciform Rhombus
2	PB01-N05 PB02-N06 PB12-N07 PB12-N08	30x40	21.40	300	0.12	Uniaxial Strong Uniaxial Weak Rhombus Quadrangular
	PB12-N17		36.30	510		Circular
3	PB01-N09 PB02-N10 PB12-N11 PB12-N12	30x50	24.39	300	0.08	Uniaxial Strong Uniaxial Weak Rhombus Quadrangular
	PB12-N18		36.30	440		Circular
4	PB01-N13 PB12-N14 PB12-N15 PB12-N16	30x30	21.57	210	0.1	Uniaxial Strong Rhombus Quadrangular Circular
5	PB12-N19 PB12-N20	30x50	43.14	300 600	0.045 0.09	Rhombus Rhombus
6	PB12-N21 PB12-N22	30x40	43.14	620	0.12	Rhombus Quadrangular
7	PB12-N23 PB12-N24	30x30	36.30	650	0.2	Rhombus Quadrangular

f_{cm} – Mean concrete compressive strength
N – Axial Load
$\nu = N/(A_c \cdot f_{cm})$ – Axial load ratio
A_c – Area of the column cross section

3. GLOBAL COLUMNS RESPONSE

From the analysis of the measured displacement and shear force paths (along the X and Y directions) are analysed. Due to the large number of tests, only a few examples of the results are presented in Figure 3, detailed information about the force-displacement results can be found in (H. Rodrigues *et al.*, 2012; Rodrigues *et al.*, 2010). From the experimental campaign the main finding were that as expected, when comparing the maximum strength in one specific direction of the columns for each biaxial test against the corresponding uniaxial test,

lower values were obtained for all biaxial tests than uniaxial ones. The biaxial loading induces a 20-30% reduction of the maximum strength of the columns in their weak direction, Y, while reductions from 8-15% for the stronger direction, X. The ultimate ductility is significantly reduced in columns subjected to biaxial load paths and the strength degradation is practically zero, in the first loading cycles, increasing after displacement ductility demands of about 3. From the strength degradation analysis, more pronounced strength degradation was observed for biaxial tests when compared with corresponding uniaxial tests.

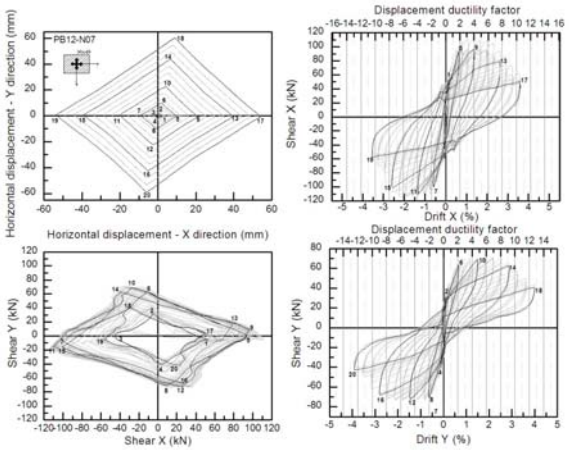

Figure 3–Global results of rectangular column PB12-N07 for rhombus load path

4. DISSIPATED ENERGY

4.1 Cumulative dissipated energy

Bousias et al. (1995) stated that the strong coupling between the two transverse directions of columns with biaxial loading produces an apparent reduction of strength and stiffness in each of the two transverse directions when considered separately, but also an increase in the hysteretic energy dissipation. This increase is due to the larger width of the hysteresis loops in the transverse direction in the presence of a non-zero force or deflection in the orthogonal direction.

The cumulative hysteretic dissipation energy was evaluated for all the tests, considering the area of each loading cycle in the X and Y direction and then the total energy was calculated as the sum of these two parts. The results in terms of evolution of cumulative dissipated energy are presented in Figure 4 for the uniaxial and biaxial tests. In Figure 4, for each displacement amplitude level, the plotted value of dissipated energy corresponds to the end of the third cycle. For the quadrangular load path, the maximum displacement for each cycle occurs in the path corner. It is also presented in the plots, along with an additional series (dashed line) representing the sum of the dissipated energy in the uniaxial tests of the corresponding column cross-section. From the analysis of the results it can be concluded:

- Comparing the two uniaxial test results, as expected a lower energy dissipation was observed for the columns tested in its weakest direction, associated with the inferior column strength in this direction (15 to 20% lower in the column of 30x40 cm^2 section and 60 to 80% in the column of 30x50 cm^2 section);
- The biaxial load paths induce larger amounts of dissipated energy than the correspondently uniaxial paths. However, the sum of the dissipated energy in the two unidirectional tests, the X and Y directions, leads to a dissipation energy evolution very close to that derived from the tests with rhombus and circular load paths;
- The quadrangular load path dissipates less energy than the other biaxial load paths. It should be recalled that that the maximum drift demands on the quadrangular load path is reached in the path corner, corresponding to $\sqrt{2}$ times the maximum drift reached along the X and Y axes. In accordance with this, the quadrangular load path dissipates 30-45% less energy when compared to the rhombus load path. However, the quadrangular load path would dissipate 40-60% more energy than the rhombus load path;
- Comparing the dissipated energy of the biaxial load paths with the sum of the dissipated energy in the two unidirectional tests, the rhombus load path tends to dissipate more than 10-20% and the circular load path dissipates more than 20-40%. The lower bound of these differences is found for the column with the square cross-section. This allows the conclusion that in the assessment and design of RC structures, not considering the bending interaction between each direction in the numerical models can introduce an error about of 10 to 40% in terms of energy dissipation.

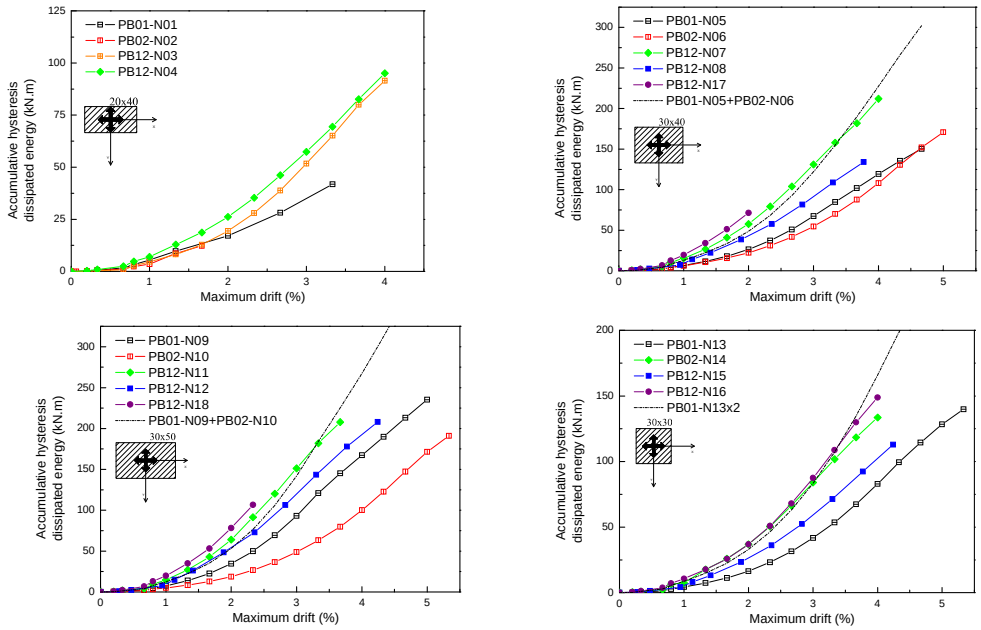

Figure 4 – Comparison of cumulative dissipated energy for columns with different load paths (uniaxial and biaxial loads)

4.2 Individual cycle energy

The energy dissipated for each individual loading cycle and the accumulated energy dissipation along each tested column was calculated (See Figure 5). For purposes of correlation, the cycles for which relevant damage states occurred during the tests were also identified, namely the reinforcement bar buckling, conventional column collapse and bar failure.

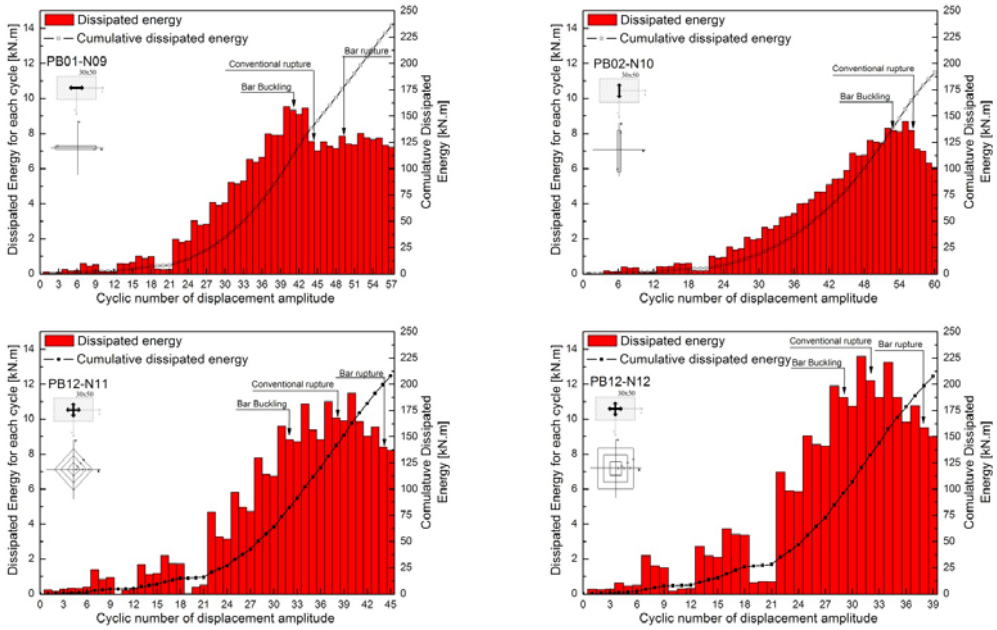

Figure 5 – Individual Cycle Energy and Cumulative Dissipated energy for a rectangular columns (N09 to N12 and N18)

In Figures 5 examples of the graphics obtained are presented. From the analysis of the results obtained for the 24 tested columns, the following can be concluded:

- In the first cycle of each peak displacement, higher energy dissipation is observed relative to the subsequent cycle with the same peak displacement. In the uniaxial tests, the reduction of the dissipated energy in the 2nd and 3rd cycles is about 10% of the energy dissipated in the 1st cycle. This reduction is more pronounced for the biaxial load path, reaching 25%. The damage induced during the first cycle

reduces the stiffness and strength, reducing the energy dissipation capacity of the column in the second and third cycles (see examples in Figure 5);

- A significant drop in the energy dissipation is observed after reaching the conventional rupture of the column. This effect is associated with the longitudinal bars buckling, which induces a high level of column strength degradation.

4.3 Total dissipated energy until conventional collapse

According to Ohno and Nishioka (Ohno & Nishioka, 1984) the total dissipated energy of a RC column is independent of the loading path. This finding is in agreement with that of Tsuno and Park (Tsuno & Park, 2004). However, in both studies the columns tested were all square columns (40x40 cm^2 and 55x55 cm^2 respectively) and with axial load stresses between 0.98 and 1.96 MPa.

Figure 6 compares the total dissipated energy obtained from the test results. This total dissipated energy corresponds to the energy dissipated from the start of the test until conventional rupture is reached, referring a strength decay of 20% relative to the maximum strength (Park & Ang, 1985). From the analysis of the results, the following observations can be drawn:

- For square columns (N13 to N16) tested with a axial load stress of 2.33 MPa, the results obtained are in agreement with those reported by Ohno and Nishioka (1984) and by Tsuno and Park (Tsuno & Park, 2004), i.e. the dissipated energy up until conventional rupture is approximately the same (see Figure 6) with differences lower than 10%. However, for square columns (N23 and N24) with a higher level of axial load stress of 7.33 MPa this conclusion is not valid (see Figure 6). The increase in axial load stress influences the total energy dissipated;
- For rectangular columns, the finding of Ohno and Nishioka (Ohno & Nishioka, 1984) is not valid (see Figure 6), the differences in strength and stiffness of the two orthogonal directions induce differences that cannot be dissociated from the biaxial coupling effect;
- Uniaxial tests in rectangular columns tested, for the same loading history (comparing N05 with N06 and N09 with N10), show that the dissipated energy up until conventional rupture is dependent of the loading direction. The total dissipated energy in the weaker direction of the column at the point of rupture is 90% (N06) and 20% (N10) higher than the corresponding results for the tests in the strong direction (N05 and N09);

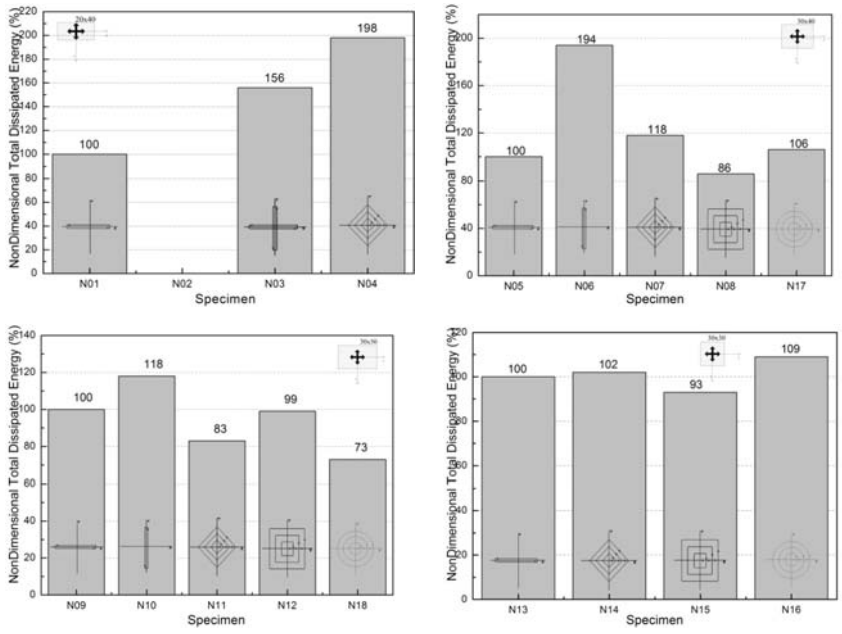

Figure 6 – Evaluation of total energy dissipated of columns tested for uniaxial and biaxial loads (with different load paths)

4.4 Normalised dissipated energy vs displacement ductility

As stated by Elmenshawi and Brown (Elmenshawi & Brown, 2010), the relation between a RC element's displacement ductility and dissipated energy is complex due to the sensitivity of both factors to the element variables. For each column tested, the calculated energy dissipation evolution was normalised with the total dissipated energy until the first yield point (E_y) until the column conventional failure, i.e. for a strength decay of 20% relative to the maximum strength.
In Figure 7, the evolution of the normalised dissipated energy as a function of the corresponding displacement ductility for the tested columns is represented. Results from the uniaxial and biaxial tests are represented with different mark filling.
The best-fit power correlation curve for all tests results (uniaxial and biaxial) is shown in Figure 7 and is given by expression 1.

$$\frac{E_{cum}}{E_y} = 0.64\mu^{2.1} \quad (1)$$

This expression is very similar to that obtained by best-fit correlation to the test results from the uniaxial and biaxial loading separately.
As given by the proposed equation, for a displacement ductility of 4 (corresponding to the minimum required ductility to withstand a severe earthquake), the corresponding normalised dissipated energy estimated is 12. Elmenshawi and Brown (Elmenshawi & Brown, 2010) and Nmai and Darwin (Nmai & Darwin, 1984) have investigated this relationship for beams (with zero axial force), proposing similar equations. From this expression a value of normalised dissipated energy for the same displacement ductility is 3 time higher, around 35. This difference can be associated with the axial loading levels.
As stated by Darwin and Nmai (Darwin & Nmai, 1986), the proposed equations need to be verified with other experimental results. A validated expression can be very useful to estimate the dissipated energy in the seismic design of RC elements in accordance with international codes such as ACI 318-08 (ACI318-08, 2008).

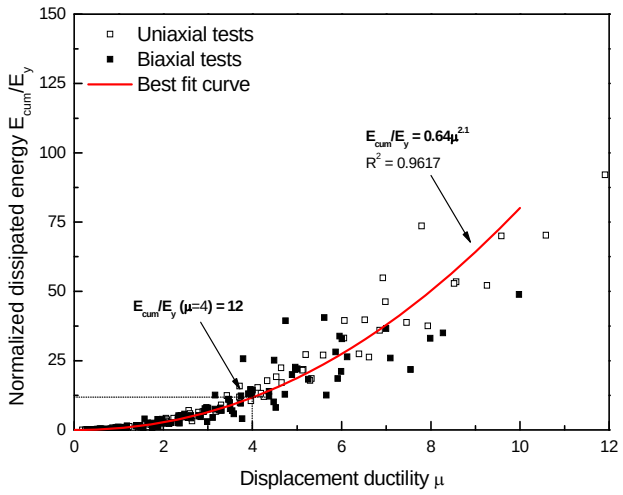

Figure 7 – Normalised dissipated energy vs displacement ductility

5. EQUIVALENT VISCOUS DAMPING RATIO

5.1 Evaluation of equivalent damping from experimental results

The equivalent damping depends on the structural displacement ductility demand and the location of the plastic hinges in the elements (Priestley, 1997). It may be interpreted as the superposition of the elastic and hysteretic damping
It is widely accepted that, for typical RC structures, the elastic damping ratio (ξ_{el}) is generally taken as 5% of the critical damping (Priestley *et al.*, 2007) and computed proportionally either to the initial (or tangent) stiffness, or to the mass, or to both stiffness and mass. By contrast, the hysteretic damping (ξ_{hyst}) depends essentially on the post-yielding characteristics of the element and it is normally taken defined proportionally to the secant stiffness (Otani, 1981), which is directly related to the hysteretic rules generally calibrated to represent the structural

response in the inelastic phase (M.J.N.Priestley *et al.*, 2005). Therefore, both damping types should not be directly summed up.
For a perfectly symmetric hysteretic response and corresponding closed loop (as in the case of pure harmonic loading), the hysteretic equivalent damping coefficient (ξ_{hyst}) can be given accurately given by the well known Expression 2, where E_D stands for the dissipated energy within a given cycle, A_{loop} is the area of the corresponding closed loop in the total restoring force - displacement diagram and E_{S0} is the "elastic" strain energy associated with the maximum force (F_{max}) and displacement (D_{max}) reached in the loop.

$$\xi_{hyst} = \frac{E_D}{4\pi E_{S0}} = \frac{A_{loop}}{2\pi F_{max} D_{max}} \quad (2)$$

However, in the case of seismic loads or even for tests performed under displacement controlled conditions, some asymmetries can be observed and the loops may not be closed, which means that the direct use of Expression 2 is less appropriate.
Therefore, based on the work of Jacobsen (Jacobsen, Steady Forced Vibrations as Influenced by Damping) and according to the procedure proposed by Varum (Varum, 2003), the equivalent hysteretic damping can be evaluated for each half-cycle of the force-displacement curves as shown in Figure 8 and described next:

- First, each half-cycle is identified, delimited by a pair of zero-force points;
- For each force-displacement half-cycle, the maximum generalised force (F_{max}) and the maximum generalised displacement (D_{max}) are evaluated, which allows calculating the "elastic" strain energy (E_{S0});
- For each half-cycle, the dissipated energy (E_D) is computed by performing the integral of the force-displacement curve leading to the $A_{half\text{-}loop}$ value;
- Finally, the equivalent damping ratio (ξ_{eq}) is computed with the Equation 3, for each half-cycle.

$$\xi_{hyst} = \frac{1}{\pi} \frac{A_{half-loop}}{F_{max} D_{max}} \quad (3)$$

This evaluation may be used as a first approach for estimating the hysteretic damping, and for comparing the tested columns with different cross sections and for different load paths. However, as pointed out by Dwairi *et al.* (Dwairi *et al.*, 2007), it should be noted that an overestimation of the equivalent damping may be obtained, when it is computed proportionally to the dissipated energy and the ductility level.

For each column tested, with a uniaxial or biaxial load path, the equivalent damping was calculated, according to the methodology presented, for each independent direction (X and Y) from the shear-drift curves. Subsequently a best-fit logarithmic curve was adjusted for each tested column in terms of equivalent damping as a function of maximum ductility demand. The best-fit logarithmic curves were for each tested column for each direction (X and Y) are compared and the equations and the correlation factors (R^2). From the analysis of the results in terms of the equivalent damping function of ductility for the different load paths allows to conclude that the a significant influence of the load path on the equivalent damping was found. Generally, the biaxial load path induces higher equivalent damping values when compared with the uniaxial tests.

5.2 Empirical proposals for equivalent damping in RC elements under uniaxial loadings

Different proposals for the equivalent damping of RC elements and structures can be found in the literature, Blandon (Blandon, 2004) developed an extensive review and study of the existing proposals for all type of elements. From an analysis of the results, from the uniaxial results the proposals of Kowalsky (Kowalsky, 1994), Priestley (Priestley, 1997) and Priestley et al.(Priestley *et al.*, 2007) present a better correlation to the experimental results, as represented in Figure 9.

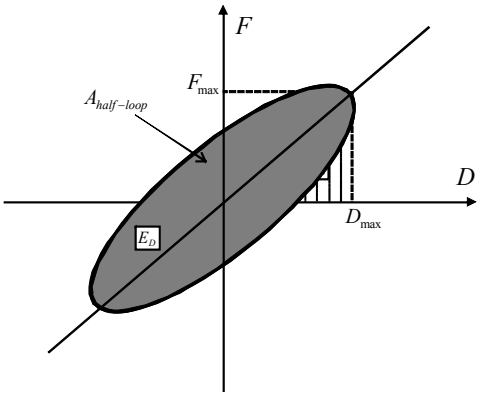

Figure 8 – Damping for a hysteretic half-cycle

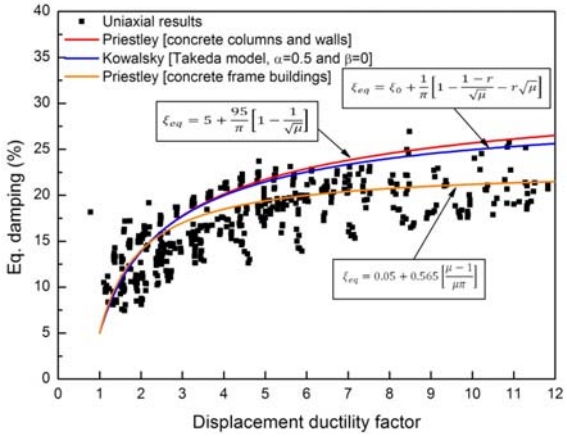

Figure 9 – Equivalent damping estimated with empirical expressions for all uniaxial tests

5.3 Equivalent biaxial damping

The equivalent damping was computed for each biaxial test, as a function of the effective damping estimated for each independent direction weighted with the respective potential energy, given by Equation 16

$$\xi_{eq} = \frac{\xi_x \cdot E_x + \xi_y \cdot E_y}{E_x + E_y} \quad (4)$$

where ξ_{eq} is the equivalent damping of the biaxial response, ξx and ξy are the equivalent damping estimated for each individual direction (X and Y) and Ex and Ey are the potential energy in each direction.
In Figure 10, the global equivalent damping obtained, according to the given methodologies, are illustrated for each load path type. The empirical expressions with better correlation to the uniaxial test results are also highlighted. From the analysis of Figure 10, the following can be concluded:

- The estimated equivalent global damping for biaxial tests is clearly dependent on the load path. For example, for a ductility factor of 2 the rhombus load path has an equivalent damping of around of 10%, while quadrangular and circular paths have an equivalent damping of 20%;
- Comparing the results obtained for uniaxial and biaxial load paths, the cruciform and rhombus paths presents similar equivalent global damping. However, the quadrangular and circular paths present higher levels of damping when compared to that obtained from the uniaxial tests. For example, for a ductility factor of 6 the uniaxial load paths induce an equivalent damping of around 20%, while for the quadrangular an equivalent damping of around 30% is observed.

From the previous comments, it is concluded that the typically used equations to estimate equivalent damping for uniaxial stress cannot be used for equivalent damping in biaxial loading conditions. However, for displacement biaxial paths close to the cruciform and rhombus the empirical equations present acceptable results.
Fardis and Panagiotakos (Fardis & Panagiotakos, 1996), from an analysis of test results of 46 columns, have confirmed that biaxial loading achieves higher values of hysteretic damping when compared to uniaxial loading. Bousias et al. (Bousias *et al.*, 1995) stated that the higher damping observed for biaxial loading is attributed to the coupling response of the columns between the two transverse directions.
Even if recognized the expressive dispersion of the viscous damping calculated from biaxial tests, were adjusted, by fitting the experimental data, different equations. The two best-fitting equations found are presented in Figure 11 (Expressions 5 and 6). Both equations have a correlation factor relative to the experimental results (R^2) of 0.31.

$$\xi_{eq} = 33.6 - \frac{22.25}{\mu^{0.87}} \quad (5)$$

$$\xi_{eq} = 12.56 + 5.18 \cdot \ln \mu \quad (6)$$

The low correlation factor found, justified by the dispersion of the equivalent damping determined from biaxial tests, is particularly dependent on the load path. However, the proposed equation can be considered as a first estimation of the equivalent damping for RC columns under biaxial loading.

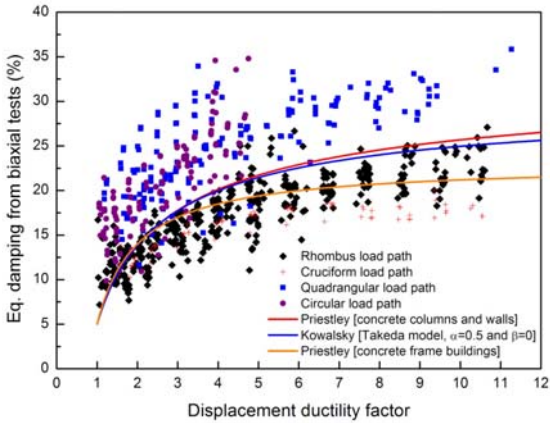

Figure 10 –Equivalent damping for biaxial tests

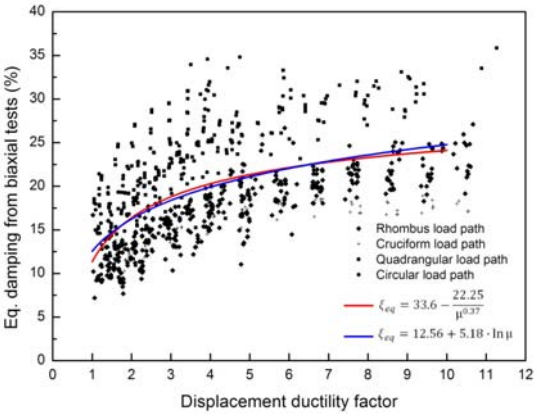

Figure 11 – Best fitted proposals for biaxial equivalent damping

6. CONCLUSIONS

An experimental campaign was carried out on 24 RC columns with different geometries and reinforcement, subjected to uniaxial and biaxial horizontal displacement paths combined with constant axial load and focusing on the study of the energy dissipation evolution and damping capacity. Based on the results, the following conclusions can be drawn:

- It was observed that biaxial loading can introduce higher energy dissipation (circular, rhombus and cruciform load paths) than uniaxial loading, as previously recognised by other authors. It was confirmed that the energy dissipation also depends on the column's geometry. For a specific imposed maximum drift, among the load paths considered in this study, the circular path was shown to be the most dissipative and the quadrangular load path the less dissipative. The quadrangular load path dissipates even less energy for a certain drift demand than the sum of the dissipated energy in two independent unidirectional tests for the corresponding drift level;
- In the first cycle of each peak displacement level, higher energy dissipation is observed than in the subsequent cycles for the same peak displacement. This effect is more pronounced in the biaxial loading tests. After reaching the conventional rupture of the column, the energy dissipated exhibits a deceleration;
- The cross-section geometry, axial load ratio and number of cycle repetitions has a significant influence on the total energy dissipation;

From the analysis of the viscous damping of each independent direction of columns when tested biaxially, a larger dispersion of the damping in each direction was found;

- However, it was verified that the viscous damping highly depends on the biaxial load path. The repetition of cycles, for the same maximum displacement level, has practically no influence on the equivalent damping;
- Different proposals, already available in the literature, for the prediction of equivalent damping of RC columns under uniaxial loading were compared with the experimental results obtained from the uniaxial tests, showing that some of these expressions do not adequately represent the results obtained;
- The equivalent biaxial damping was computed with the results of each biaxial test, presenting a huge dispersion. The equivalent biaxial damping is highly dependent on the load path;

A large number of questions are still open concerning the biaxial behaviour of RC columns, especially regarding equivalent viscous damping associated with loading path. In the present work, the expressions proposed relating the normalised dissipated energy and equivalent biaxial damping with displacement ductility constitutes a preliminary step towards this goal. However these expressions need to be checked against additional experimental results. Even so, the research work reported is expected to contribute towards a better understanding of the biaxial response of RC columns and for the calibration of suitable numerical models for the representation of the biaxial lateral response of reinforced concrete columns under cyclic loading reversals.

ACKNOWLEDGMENTS

The authors acknowledge to the LESE laboratory staff, particularly Valdemar Luís, André Martins and Engº Luís Noites, for all the support in the preparation and implementation of the testing set-up. This paper reports research developed under financial support provided by "FCT - Fundação para a Ciência e Tecnologia", Portugal, namely through the PhD grants of the first author with reference SFRH/BD/63032/2009, and through the research project PTDC/ECM/102221/2008.

REFERENCES

ACI318-08. (2008). Building code requirements for structural concrete (ACI 318-08) and commentary (ACI 318R-08): USA: American Concrete Institute.

Blandon, C. (2004). *Equivalent Viscous Damping Equations for Direct Displacement Based Design.* Master, Rose School, Pavia.

Bousias, S. N., Verzeletti, G., Fardis, M. N., & Gutierrez, E. (1995). Load-path effects in column biaxial bending with axial force. *Journal of Engineering Mechanics*, 596-605.

CEB. (1996). RC frames under earthquake loading. Lausanne.

Darwin, D., & Nmai, C. K. (1986). Energy Dissipation in RC Beams Under Cyclic Load. *Journal of Structural Engineering, 112*(8), 1829-1846.

Dwairi, H. M., Kowalsky, M. J., & Nau, J. M. (2007). Equivalent Damping in Support of Direct Displacement-Based Design. *Journal of Earthquake Engineering, 11*(4), 512-530. doi: 10.1080/13632460601033884

Elmenshawi, A., & Brown, T. (2010). Hysteretic energy and damping capacity of flexural elements constructed with different concrete strengths. [doi: DOI: 10.1016/j.engstruct.2009.09.016]. *Engineering Structures, 32*(1), 297-305.

Fardis, M., & Panagiotakos, T. (1996). *Hysteretic damping of reinforced concrete elements*. Paper presented at the 11th World Conference on Earthquake Eng, Acapulco, Mexico.

H. Rodrigues, A. Arêde, H. Varum, & A.G. Costa. (2012). Experimental evaluation of rectangular reinforced Concrete column behaviour under biaxial cyclic Loading. *Earthquake Engineering and Structural Dynamics (in press)*.

Jacobsen, L. S. (Steady Forced Vibrations as Influenced by Damping). 1930. *ASME Transactione 52*(1), 169-181.

Kowalsky, M. J. (1994). *Displacement based design-A methodology for seismic design applied to RC bridge columns.* MSc Thesis, University of California, San Diego, California.

Lu, B., & Silva, P. F. Estimating equivalent viscous damping ratio for RC members under seismic and blast loadings. [doi: DOI: 10.1016/j.mechrescom.2006.05.002]. *Mechanics Research Communications, 33*(6), 787-795.

M.J.N.Priestley, D.N.Grant, & C.A.Blandon. (2005). *Direct displacement-based seismic design*. Paper presented at the Proceedings of the New Zealand Society for Earthquake Engineering Conference, Wairakei, New Zealand.

Nmai, C. K., & Darwin, D. (1984). Cyclic behavior of lightly reinforced concrete beams. University of Kansas Centre for Research, SM report no. 12.

Ohno, T., & Nishioka, T. (1984). An experimental study on energy absorption capacity of columns in reinforced concrete structures. *Proceedings of the JSCE, Structural Engineering/Earthquake Engineering, 1, No 2*, 137-147.

Otani, S. (1981). Hysteresis models of reinforced concrete for earthquake response analysis. *Journal of Faculty of Engineering, 36, No. 2*, 407 – 441.

Park, Y. J., & Ang, H. S. (1985). Seismic Damage Model for Reinforced Concrete. *ASCE - J Struct Eng, 111(4)*, 722-739.

Priestley, M. J. N. (1997). Displacement-based seismic assessment of reinforced concrete buildings. *Journal of Earthquake Engineering - Imperial College of London, 1*(1), 157-192.

Priestley, M. J. N., Calvi, G. M., & Kowalsky, M. J. (2007). *Direct Displacement-Based Seismic Design of Structures*: IUSS Press, Pavia.

Rodrigues, H., Arêde, A., Varum, H., & Costa, A. G. (2010). *Experimental study on the biaxial bending cyclic behaviour of RC columns*. Paper presented at the 14th European Conference on Earthquake Engineering Ohrid, Republic of Macedonia.

Tsuno, K., & Park, R. (2004). Experimental study of reinforced concrete bridge piers subjected to bi-directional quasi-static loading. *Struct. Engrg Structures, JSCE, 21, No 1 11s-26s*.

Varum, H. (2003). *Seismic assessment, strengthening and repair of existing buildings.* PhD Thesis, University of Aveiro, Aveiro.